

## Solution-processed poly(3-hexylthiophene) vertical organic transistor

Sheng-Han Li, Zheng Xu, Guanwen Yang, Liping Ma, and Yang Yang<sup>a)</sup>

*Department of Materials Science and Engineering, The Henry Samueli School of Engineering and Applied Science, University of California, Los Angeles, California 90095, USA*

(Received 27 June 2008; accepted 25 October 2008; published online 25 November 2008)

The fabrication and operation of a solution-processed vertical organic transistor are now demonstrated. The vertical structure provides a large cross section and a short channel length to counter the inherent limitations of the organic materials. The operation of a vertical organic transistor relies on a transition metal oxide layer,  $V_2O_5$ , to lower the carrier injection barrier at the organic/metal interface. The effect of the oxide thickness was examined to verify the role of transition metal oxide in device operation. By studying the device performance at different temperatures and in solvent environments, an operating mechanism that occurs via an ion drift and doping process was proposed. The drift direction of the dissolved  $Li^+$  ion can be controlled by altering the gate voltage bias in order to change the carrier injection barrier. © 2008 American Institute of Physics. [DOI: 10.1063/1.3030990]

After decades of research and development, organic semiconductors have attracted extensive interest in electronic device applications such as organic light emitting diodes,<sup>1-3</sup> field-effect transistors in both lateral<sup>4-6</sup> and vertical structures,<sup>7-9</sup> memory,<sup>10,11</sup> and photovoltaics.<sup>12-14</sup> Polymer based organic semiconductors are attractive due to their processing advantages. For low cost and large area organic electronic devices, solution processing offers a powerful method for embedding electronic functionality into substrates.<sup>15</sup> However, because of the inherent limitation of organic semiconductors, the mobility and device output current are insufficient for commercial applications. One approach to enhance the output current is utilizing a polymer electrolyte dielectric layer with a high capacitance (greater than  $10 \mu F/cm^2$ ).<sup>16,17</sup> The benefits of this electrolyte dielectric layer are (1) higher output currents and (2) lower operating gate voltages. Another approach is to change the current flow direction from lateral to vertical to obtain large currents and low operating voltage.

In this letter, we demonstrate a solution-processed vertical organic transistor with a transition metal oxide (TMO) layer serving as a charge injection layer. This device can operate at a low voltage with high current output. By studying device performance at different temperatures and in different solvent environments, we propose an operating mechanism for the vertical organic field effect transistor (VOFET). A solution processed polymer VOFET device contains two connected cells: the capacitor and semiconductor cell [Fig. 1(a)]. The middle electrode is defined as the common-source electrode, which is thin and has rough morphology. Aluminum (Al) used in conjunction with a TMO layer is used as the source electrode to ensure a suitable barrier to prevent charge injection at zero gate voltage. The top and bottom electrodes are defined as the gate and drain, respectively. In this letter, 35 nm of Al was deposited onto a pre-cleaned glass substrate as the bottom gate electrode. Afterward, a 200 nm lithium fluoride (LiF) layer was deposited as the gate dielectric layer on top of the Al layer. Then, the source electrode was deposited using an Al with 17 nm thickness. Various charge injection layer ( $V_2O_5$ ) thicknesses

were deposited on top of the source electrode surface. After charge injection layer deposition, we transferred the glass slide into a dry box where the oxygen and moisture level were below 0.1 ppm. A thin polymer semiconductor film was deposited through spin coating of a chloroform solution of 2 wt % poly(3-hexylthiophene) (P3HT); the P3HT and chloroform were purchased from Rieke Metals, Inc. and Sigma-Aldrich, respectively, and used without further purifications. Finally, the sample was transferred into the vacuum chamber for top electrode deposition. A 35 nm aluminum film was deposited onto the organic cell surface as the drain electrode. The device area was  $2.4 \text{ mm}^2$ , as defined by the crossover area between the drain and source electrodes. In order to investigate the operating mechanism and the device performance at different temperatures, we encapsulated the devices using cover glass slides and UV-cured epoxy. After the curing process, we transferred the devices into a temperature controllable probe station at a pressure of  $1 \times 10^{-5}$  Torr. The IV characterization was performed using an HP 4155B semiconductor parameter analyzer.

The most important concept concerning the vertical organic transistor is the control of charge injection, in particular, hole injection from the source electrode to the organic layer. The work function of Al,  $V_2O_5$ , and the highest occupied molecular orbital (HOMO) and lowest unoccupied molecular orbital (LUMO) levels of P3HT are shown in the energy level diagram [Fig. 1(b)]. The output characteristics of the vertical organic transistor when operated inside the dry box (the oxygen and water concentration are both below 1 ppm) do not show any transistor behavior, i.e., the source-drain current ( $I_{SD}$ ) maintains the same value with different applied gate bias [Fig. 1(c)]. The  $I$ - $V$  properties indicate that the hole injection barrier between the  $V_2O_5$  coated Al electrode and P3HT is unchanged. Figure 1(d) shows the output characteristics of the same device tested under the ambient condition, relative humidity of 45%. In the presence of humidity, this device had significant transistor properties near 0.4 mA output current and a  $10^3$  on/off ratio (current ratio at certain drain voltage with and without gate bias at  $-5 \text{ V}$ ).

The influence of the charge injection layer,  $V_2O_5$ , can be explained by the TMO layer thicknesses and output current dependence. According to the energy diagram, without TMO

<sup>a)</sup>Electronic mail: yangy@ucla.edu.

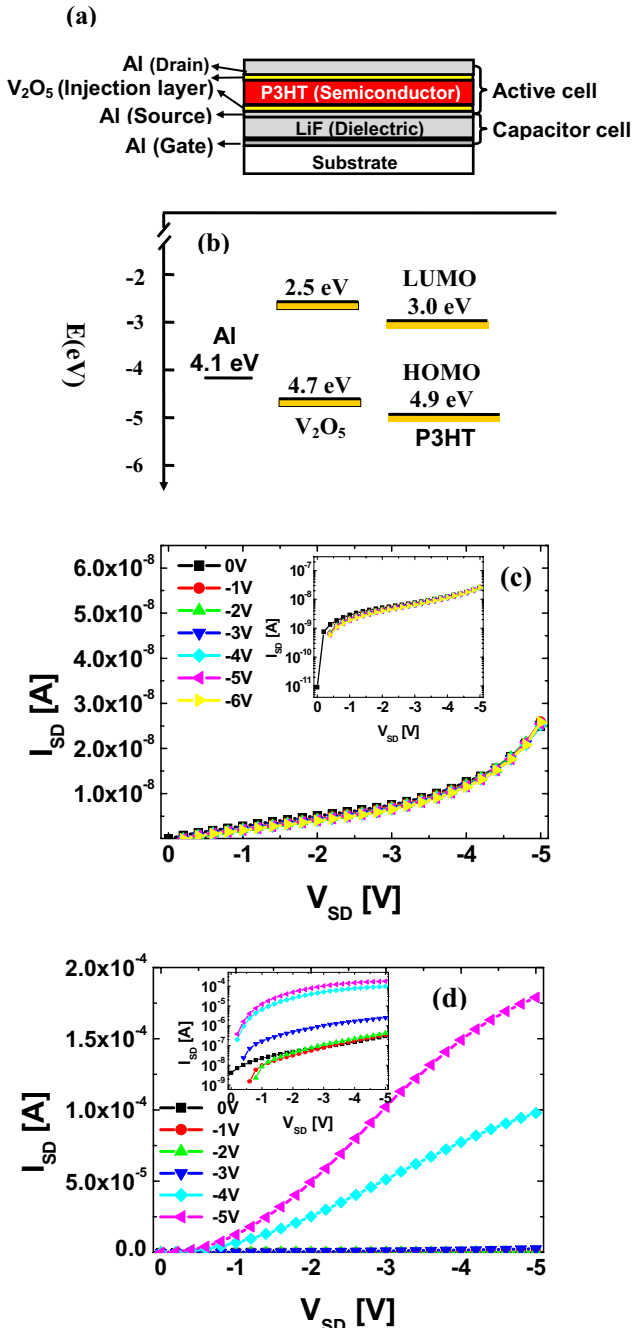


FIG. 1. (Color online) (a) A schematic cross section of the polymer vertical organic transistor structure. (b) Energy diagram of the work function of Al, V<sub>2</sub>O<sub>5</sub>, and the HOMO and LUMO levels of P3HT. (c) Output characteristics of the device tested inside a dry box (oxygen and moisture level are below 0.1 ppm). The inset figures depict a logarithm scale used to extract the device ON/OFF ratio. (d) Output characteristics of the polymer device tested under the ambient conditions (relative humidity of about 30%–40%).

layer, the hole injection barrier between Al and P3HT (0.8 eV) is too large and cannot be sufficiently modified by the gate bias. Therefore, transistor behavior cannot be observed for Al-only source electrode devices [Fig. 2(a)]. When a 2.5 nm thick V<sub>2</sub>O<sub>5</sub> layer was inserted between the Al source electrode and the P3HT layer, the source electrode surface was not fully covered by V<sub>2</sub>O<sub>5</sub>. As a result, the effective area (the area covered by V<sub>2</sub>O<sub>5</sub>) for hole injection is small. Therefore, only a small amount of carriers can pass through the barrier. The device with 2.5 nm TMO layer has small output current and on/off ratio of one order of magnitude [Fig.

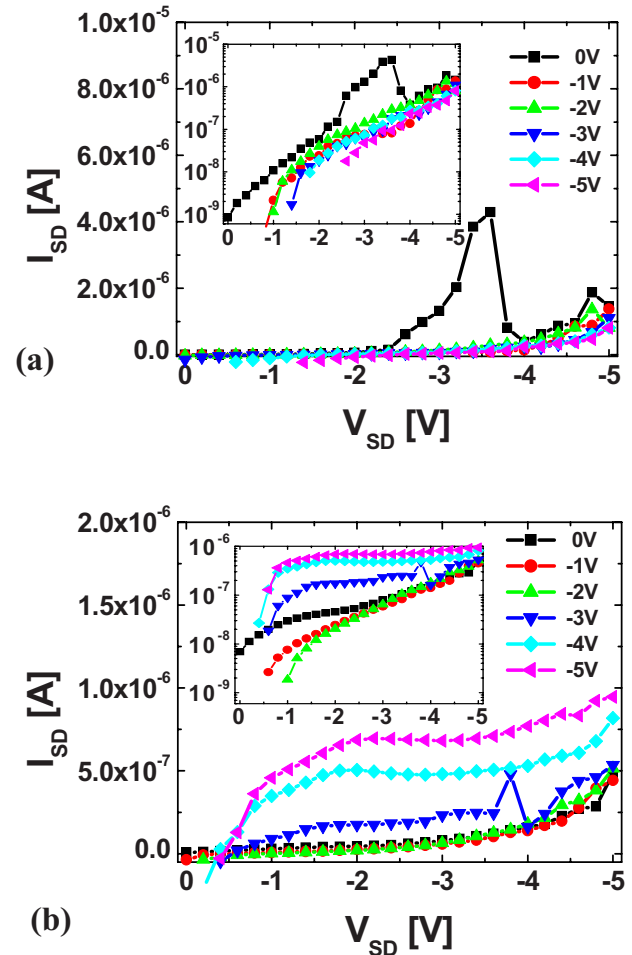


FIG. 2. (Color online) Output characteristics of the polymer vertical organic transistor with different TMO thickness tested in the ambient condition (relative humidity of about 30%–40%). The inset figures depict a logarithmic scale used to extract the device ON/OFF ratio. (a) 0 and (b) 2.5 nm.

2(b)]. When the TMO layer thickness is over 10 nm, the hole injection from the source electrode into the organic layer dominates the source-drain current leading to maximum current output [Fig. 1(d)]. As shown in Fig. 1(d), the curve  $I_{SD}$  increases from 2  $\mu$ A to 0.2 mA when the thickness of the V<sub>2</sub>O<sub>5</sub> charge injection layer is increased. This result suggests that this charge injection layer plays an important role in determining device performance. In addition, the effective area for hole injection also increases until it reaches the geometric area of the device, where  $I_{SD}$  is governed by the injection barrier between V<sub>2</sub>O<sub>5</sub> and P3HT.

The difference between the output characteristics shown in Figs. 1(b) and 1(c) indicates that water molecules play an important role in device operation. Furthermore, these experiments indicate that the device works in other polar solvents such as acetonitrile. Here, we propose a possible operating mechanism after studying the dependence of the  $I_{SD}$  on temperature in different solvent environments. As described in the previous section, P3HT devices were first packaged using epoxy and a glass cover slip in an ambient environment; thus, the absorbed water vapor was retained inside the devices. During the testing processes, the voltage difference between source and drain electrode was kept at  $-5$  V.

Figure 3 shows source-drain currents ( $I_{SD}$ ) versus experiment time in different temperature regions. At the first step, we applied voltage biases at source and gate electrodes

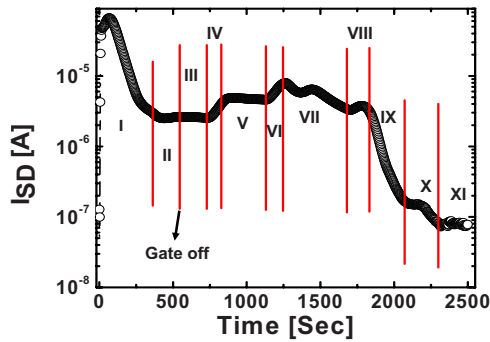


FIG. 3. (Color online) The device output currents and temperature dependence. I stage: device was quenched from 340 to 230 K. II stage: temperature held at 230 K. Gate bias was still on. III stage: gate bias was removed. The output current can reach a steady state. IV stage: increased temperature to 250 K. The current began to increase. V stage: held the temperature at 250 K. VI stage: increased temperature from 250 to 270 K. VII stage: held the temperature at 270 K. VIII stage: increased temperature from 270 to 300 K. IX stage: held the temperature at 300 K. X stage: increased temperature from 300 to 330 K. XI stage: held the temperature at 330 K.

and simultaneously lowered the temperature from 340 to 230 K with liquid nitrogen. Then, the temperature was held constant at 230 K and a steady state current output was observed. After 10 min, the gate bias was removed. The value of  $I_{SD}$  maintained at the same value as when  $I_{SD}$  was under gate bias. We believe this interesting phenomenon is caused by the drifting and doping processes of  $\text{Li}^+$ . Because of the unique discontinuous source electrode of the vertical organic transistor,<sup>18–20</sup> the LiF layer is in contact with both the source electrode and semiconductor layer. Under the ambient conditions, LiF forms the cation  $\text{Li}^+$  and the anion  $\text{F}^-$  at the junctions of the Al, LiF, and P3HT layers. Panzer and Frisbie<sup>21</sup> proposed a possible mechanism of  $\text{Li}^+$  doping in P3HT organic semiconductor films that changes the conduction behavior. Fang *et al.*<sup>22</sup> and Kaake *et al.*<sup>17</sup> also observed the same behaviors in pentacene and N–N'-dioctyl-3,4,9,10-perylene tetracarboxylic diimide field-effect transistors, respectively.<sup>3</sup> In vertical organic transistor devices, we believe that the carrier injection barrier from the source electrode to the organic layer can be modified with ions such as  $\text{Li}^+$  and  $\text{F}^-$  migrating into the semiconductor layer. The applied gate bias creates an electric field inside the dielectric layer and separates the ions. These ions will diffuse into the P3HT layer to form dopants, which will change the injection barrier, limiting the carrier transport from the source electrode to the drain electrode. By adjusting the gate bias, we can control the drifting direction of ions in order to change the injection barrier. Once the device was cooled down to 230 K, the ions remained at the same positions as when the gate bias was initially turned on. With these preoriented ion distributions, we can observe the on-state device without gate bias. At the fourth stage in Fig. 3, we increased the system temperature to 250 K.  $I_{SD}$  began to increase and then remained constant at the fifth stage. The increasing current might have been caused by the thermally excited hopping carriers. Since we can observe a large current output, the transistor was still at the on status. At the seventh stage, when the temperature reached to 270 K, the current began to decrease. This decrease in  $I_{SD}$  might indicate that the increasing injection barrier height is due to the nonaligned and more freely moving ions at the higher temperature. The ninth and tenth stages show the same behavior; however, the slope of

current is larger than in previous stages, indicating that the ions move more easily at higher temperatures.

In summary, we have studied the electronic properties of vertical polymer based transistors. The TMO layer,  $\text{V}_2\text{O}_5$ , and partial-oxidized Al were utilized to form a nanoscale composite source electrode. The role of the TMO is to reduce the hole injection barrier between P3HT and the electrode. We also examined the effect of the oxide thickness to verify the role of  $\text{V}_2\text{O}_5$  for the device. From the temperature effect study, we propose a possible operating mechanism for the vertical organic (polymer) vertical transistor: under the ambient conditions, the adsorbed water dissolves small amount of LiF, forming  $\text{Li}^+$  and  $\text{F}^-$  at the junctions of the Al, LiF, and P3HT layers. The  $\text{Li}^+$  doping of the P3HT organic semiconductor film changes the conduction behavior. In vertical organic transistors, we believe that the carrier injection barrier from the source electrode to the organic layer can be modified by ion migration into the semiconductor layer. The applied gate bias created an electric field inside the dielectric layer and caused the anions and cations to separate. These ions will then diffuse into the P3HT layer as dopants, which change the injection barrier and thus carrier transport from the source electrode to the drain electrode. By adjusting the gate bias, we can control the drifting direction of ions and effectively modulate the injection barrier.

The authors deeply appreciate the financial support provided by the U.S. Air Force Office of Scientific Research, Grant No. FA9550-07-1-0264 (Dr. Charles Lee). The authors would like to thank Dr. David Margolese of ORFID Corporation.

- <sup>1</sup>C. W. Tang and S. A. VanSlyke, *Appl. Phys. Lett.* **51**, 913 (1987).
- <sup>2</sup>J. H. Burroughes, D. D. C. Bradley, A. R. Brown, R. N. Marks, K. Mackay, R. H. Friend, P. L. Burns, and A. B. Holmes, *Nature (London)* **347**, 539 (1990).
- <sup>3</sup>J. Huang, G. Li, E. Wu, Q. Xu, and Y. Yang, *Adv. Mater. (Weinheim, Ger.)* **18**, 114 (2006).
- <sup>4</sup>H. Koezuka, A. Tsumura, and T. Ando, *Synth. Met.* **18**, 699 (1987).
- <sup>5</sup>G. Horowitz, F. Garnier, A. Yassar, R. Hajlaoui, and F. Kouki, *Adv. Mater. (Weinheim, Ger.)* **8**, 52 (1996).
- <sup>6</sup>M. Hamedi, R. Forchheimer, and O. Inganäs, *Nature Mater.* **6**, 357 (2007).
- <sup>7</sup>K. Kudo, M. Iizuka, S. Kuniyoshi, and K. Tanaka, *Thin Solid Films* **393**, 362 (2001).
- <sup>8</sup>N. Stutzmann, R. H. Friend, and H. Sirringhaus, *Science* **299**, 1881 (2003).
- <sup>9</sup>L. Ma and Y. Yang, *Appl. Phys. Lett.* **85**, 5084 (2004).
- <sup>10</sup>L. P. Ma, J. Liu, and Y. Yang, *Appl. Phys. Lett.* **80**, 2997 (2002).
- <sup>11</sup>J. Ouyang, C. W. Chu, R. J. H. Tseng, A. Prakash, and Y. Yang, *Proc. IEEE* **93**, 1287 (2005).
- <sup>12</sup>C. W. Tang, *Appl. Phys. Lett.* **48**, 183 (1986).
- <sup>13</sup>N. S. Sariciftci, D. Braun, C. Zhang, V. I. Srdanov, A. J. Heeger, G. Stucky, and F. Wudl, *Appl. Phys. Lett.* **62**, 585 (1993).
- <sup>14</sup>G. Li, V. Shrotriya, J. S. Huang, Y. Yao, T. Moriarty, K. Emery, and Y. Yang, *Nature Mater.* **4**, 864 (2005).
- <sup>15</sup>C. Y. Y. Noh, N. Zhao, M. Caironi, and H. Sirringhaus, *Nat. Nanotechnol.* **2**, 784 (2007).
- <sup>16</sup>M. Panzer and C. D. Frisbie, *J. Am. Chem. Soc.* **129**, 6599 (2007).
- <sup>17</sup>L. G. Kaake, Y. Zou, M. Panzer, and C. D. Frisbie, *J. Am. Chem. Soc.* **129**, 7824 (2007).
- <sup>18</sup>S. H. Li, Z. Xu, L. Ma, C. W. Chu, and Y. Yang, *Appl. Phys. Lett.* **91**, 083507 (2007).
- <sup>19</sup>Z. Xu, S. H. Li, L. P. Ma, G. Li, G. W. Yang, and Y. Yang, **93**, 023302 (2008).
- <sup>20</sup>Z. Xu, S. H. Li, L. Ma, G. Li, and Y. Yang, *Appl. Phys. Lett.* **91**, 092911 (2007).
- <sup>21</sup>M. Panzer and C. D. Frisbie, *J. Am. Chem. Soc.* **129**, 6599 (2007).
- <sup>22</sup>B. Fang, H. Zhou, and I. Honma, *Appl. Phys. Lett.* **89**, 023102 (2006).